Chemical Science

ROYAL SOCIETY OF CHEMISTRY

EDGE ARTICLE

View Article Online
View Journal | View Issue

Cite this: *Chem. Sci.*, 2022, **13**, 7462

All publication charges for this article have been paid for by the Royal Society of Chemistry

Received 27th April 2022
Accepted 2nd June 2022

DOI: 10.1039/d2sc02364d

rsc.li/chemical-science

Efficient visible/NIR light-driven uncaging of hydroxylated thiazole orange-based caged compounds in aqueous media†

Ryu Hashimoto,[a] Masafumi Minoshima,[a] Souhei Sakata,[b] Fumihito Ono,[b] Hirokazu Ishii,[c] Yuki Watakabe,[c] Tomomi Nemoto,[c] Saeko Yanaka,[d] Koichi Kato[d] and Kazuya Kikuchi*[ae]

In photoactivation strategies with bioactive molecules, one-photon visible or two-photon near-infrared light-sensitive caged compounds are desirable tools for biological applications because they offer reduced phototoxicity and deep tissue penetration. However, visible-light-sensitive photoremovable protecting groups (PPGs) reported so far have displayed high hydrophobicity and low uncaging cross sections ($\varepsilon\Phi$ < 50) in aqueous media, which can obstruct the control of bioactivity with high spatial and temporal precision. In this study, we developed hydroxylated thiazole orange (HTO) derivatives as visible-light-sensitive PPGs with high uncaging cross sections ($\varepsilon\Phi \approx 370$) in aqueous solution. In addition, 2PE photolysis reactions of HTO-caged glutamate were achieved using a NIR laser (940 nm). Moreover, HTO-caged glutamate can activate *N*-methyl-D-aspartic acid receptors in *Xenopus* oocytes and mammalian cells with green-light illumination, thus allowing optical control of biological functions.

Introduction

Caged compounds are powerful tools for non-invasive spatial and temporal control of bioactivity and are produced by incorporating photoremovable protecting groups (PPGs) into the structures of bioactive compounds.[1] Illumination of caged compounds leads to the immediate release of biomolecules and activation of their biofunctions. Therefore, light-induced cargo release technology has gained attention in the fields of chemical biology, photoactivated chemotherapy, and neuroscience.[2,3] As biologically useful caged compounds, they should be soluble and stable in aqueous solution and undergo efficient photorelease. Although conventional PPGs such as *o*-nitrobenzyl or coumarin-4-ylmethyl groups meet those conditions,[1] they require high-energy UV-light illumination, leading to cellular damage or death at a low tissue penetration depth.

Recently, limited numbers of visible-light-sensitive PPGs (>450 nm) based on ruthenium complexes,[4] boron dipyrromethene (BODIPY) derivatives,[5–8] or cyanine dyes[9–12] have been reported.[13] However, most of them suffer from low water solubility, which limits their manipulation in biological systems. Moreover, their uncaging cross sections (uncaging efficiencies) were measured in organic solvents, which could have affected the uncaging of biomolecules under physiological conditions. While some BODIPY-based PPGs displayed improved water solubility,[14] their uncaging cross sections and water solubility were still low ($\varepsilon\Phi \approx$ 3–24 in CH_3CN/water (7/3)).

Compared with one-photon excitation (1PE), two-photon excitation (2PE) with near-infrared light (NIR) provides deeper tissue penetration, diminished phototoxicity, and high 3D resolution.[15,16] Most 2PE-sensitive PPGs are activated by 740–800 nm light since they absorb UV/blue light whereas only a few 2PE-sensitive caged compounds[17] are active at longer than 900 nm. Uncaging with long-wavelength two-photon light enables an extra level of spatial and temporal control in deeper tissues. Although optical control with long-wavelength light is highly demanded for a wide range of biological applications such as control of neural activity in neuroscience and drug release in photoactivated chemotherapy, the development of visible/NIR light-sensitive PPGs with high uncaging cross sections in aqueous solution is still highly challenging.

Here, we present new visible/NIR light-sensitive PPGs for caged compounds with high uncaging cross sections in aqueous

[a]*Division of Applied Chemistry, Graduate School of Engineering, Osaka University, 2-1 Yamadaoka, Suita, Osaka, 565-0871, Japan. E-mail: kkikuchi@mls.eng.osaka-u.ac.jp*
[b]*Department of Physiology, Faculty of Medicine, Osaka Medical and Pharmaceutical University, 2-7, Daigakucho, Takatsuki, Osaka, 569-8686, Japan*
[c]*Exploratory Research Center on Life and Living Systems (ExCELLS), National Institute for Physiological Sciences (NIPS), National Institutes of Natural Sciences, 5-1 Higashiyama, Myodaiji, Okazaki, 444-8787, Japan*
[d]*Exploratory Research Center on Life and Living Systems (ExCELLS), Institute for Molecular Science (IMS), National Institutes of Natural Sciences, 5-1 Higashiyama, Myodaiji, Okazaki, 444-8787, Japan*
[e]*Immunology Frontier Research Center, Osaka University, 2-1 Yamadaoka, Suita, Osaka, 565-0871, Japan*

† Electronic supplementary information (ESI) available. See https://doi.org/10.1039/d2sc02364d

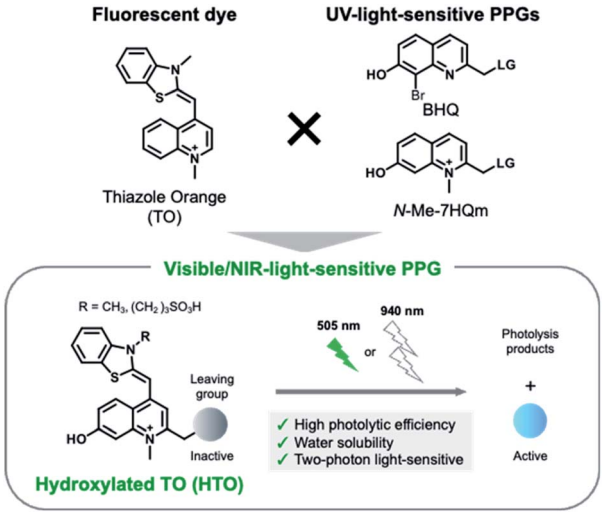

Fig. 1 Design of hydroxylated TO (HTO)-based PPGs.

solution. We developed hydroxylated thiazole orange (HTO) dye-based PPGs which absorb visible green light (Fig. 1). Caged compounds with HTO-based PPGs were efficiently uncaged by green-light illumination under physiological conditions and were stable under dark conditions. In addition, 2PE photolysis reactions of HTO-caged glutamate (**Sul-HTO-Glu**) were achieved using an NIR laser (940 nm). Finally, we proved visible-light activation of *N*-methyl-D-aspartic acid receptors (NMDARs) with **Sul-HTO-Glu** in *Xenopus* oocytes and mammalian cells. We envision that HTO-caged compounds can be used as new photochemical tools for the manipulation of biological functions using one-photon visible or two-photon NIR light excitation.

Results and discussion

Design, synthesis, and photochemical properties of HTO-caged compounds

We designed visible-light sensitive PPGs based on hydroxylated thiazole orange (HTO) using thiazole orange (TO) as the molecular framework of the chromophore (Fig. 1). TO absorbs visible green light with a high absorption coefficient and is used as a fluorescent dye for nucleic acid staining.[18] In addition, this dye contains a quinoline/*N*-methylquinolinium moiety that serves as a scaffold for UV light-sensitive PPGs.[19–22] Photo-induced deprotonation of the 7-hydroxyl group of quinoline-based PPGs accelerates the intramolecular charge transfer excited state, resulting in bond dissociation at the 2-methyl position with a high quantum efficiency of 1PE and 2PE.[23,24] Although 7-hydroxylquinoline-based PPGs are photolyzed with high uncaging cross sections to 1PE and 2PE, they have low molar absorption coefficients in short-wavelength regions (365 nm for 1PE or 740 nm for 2PE).[22] In contrast, in our molecular design of HTO, a 7-hydroxylquinoline-based PPG is incorporated into TO that has a high absorption coefficient in the visible light region. Furthermore, hydrophilic groups can be introduced into the HTO scaffold, which improves its water solubility. Thus, we reasoned that HTO-based PPGs would enable visible-light uncaging with high uncaging cross sections in aqueous solution.

Photoactivation of HTO by green light was assessed using synthetic model caged compounds bearing acetic acid (**HTO-OAc**) and piperonylic acid (**HTO-OPip**) as leaving groups (Fig. 2). Methoxymethyl (MOM)-protected 7-hydroxyquinoline derivatives were conjugated with leaving groups, followed by *N*-alkylation. After the formation of TO analogs with 2,3-dimethylbenzo[*d*]thiazol-3-ium, the target compounds were obtained by deprotection of MOM groups (Schemes S1 and S2†).

HTO-OAc and **HTO-OPip** showed no hydrolysis for 24 h under dark conditions (Fig. S2†). The time courses for the one-photon photolysis reactions of **HTO-OAc** or **HTO-OPip** with internal standards were monitored by HPLC analysis (Fig. 2). Illumination of **HTO-OAc** in aqueous solution with green light led to rapid degradation of **HTO-OAc** (Fig. 2c and d). The photo-induced release of acetic acid from **HTO-OAc** was monitored using ^{1}H-NMR (Fig. S4†). In the case of **HTO-OPip**, the released product, piperonylic acid, was detected by HPLC after green light illumination (in PBS buffer/MeCN = 1 : 1, 3% DMSO) (Fig. 2g). Illumination of **HTO-OPip** resulted in an 80% theoretical yield of piperonylic acid (Fig. 2h). However, **HTO-OPip** showed slower degradation than **HTO-OAc**. This result indicates the solvent dependency of uncaging of HTO derivatives and is consistent with the effects observed when an aprotic polar solvent (acetonitrile) was used with quinoline-based PPGs.[24] Further investigation of the photolysis mechanism of the HTO scaffold is shown in the ESI (Fig. S6–S8).†

The molar absorption coefficients (ε), photolysis quantum yields (Φ), and uncaging cross sections ($\varepsilon\Phi$) are summarized in Table 1. The uncaging cross section of **HTO-OAc** in aqueous solution was 370. This value is approximately five times higher than that of the BODIPY-core PPG ($\varepsilon\Phi = 70$ in methanol) bearing the same leaving group (acetic acid).[7] The high uncaging cross section was attributed to higher Φ values for **HTO-OAc** compared with BODIPY-based PPGs ($\Phi = 4$–24×10^{-4} in methanol),[7] while the ε values are in the same order of magnitude. This result indicates that HTO-caged compounds have superior properties for spatial and temporal control of biological functions compared to BODIPY-based visible-light-sensitive PPGs.

HTO-caged glutamate

Next, we developed HTO-caged glutamate for activation of neurotransmitters with visible/NIR light. UV-light and two-photon activatable caged glutamates have been widely used in neuroscience to control neuronal activity.[25] However, no caged glutamate that undergoes one-photon uncaging with longer-wavelength light (>500 nm) exists. For two-photon uncaging, only DEAC450 has been reported to be a two-photon-activatable caged glutamate at ~900 nm.[17] We assumed that the high uncaging cross sections of HTO were suitable for the development of long wavelength-light sensitive caged glutamate. Therefore, we designed HTO-caged glutamate (**Sul-HTO-Glu**) (Fig. 3a). In the molecular design of **Sul-HTO-Glu**, a sulfonic acid is introduced from the benzothiazole nitrogen of the HTO scaffold, which can enhance the water solubility.

As expected, **Sul-HTO-Glu** did not aggregate, even in PBS buffer containing 0.1% DMSO (Fig. 3b and S1†). Illumination of

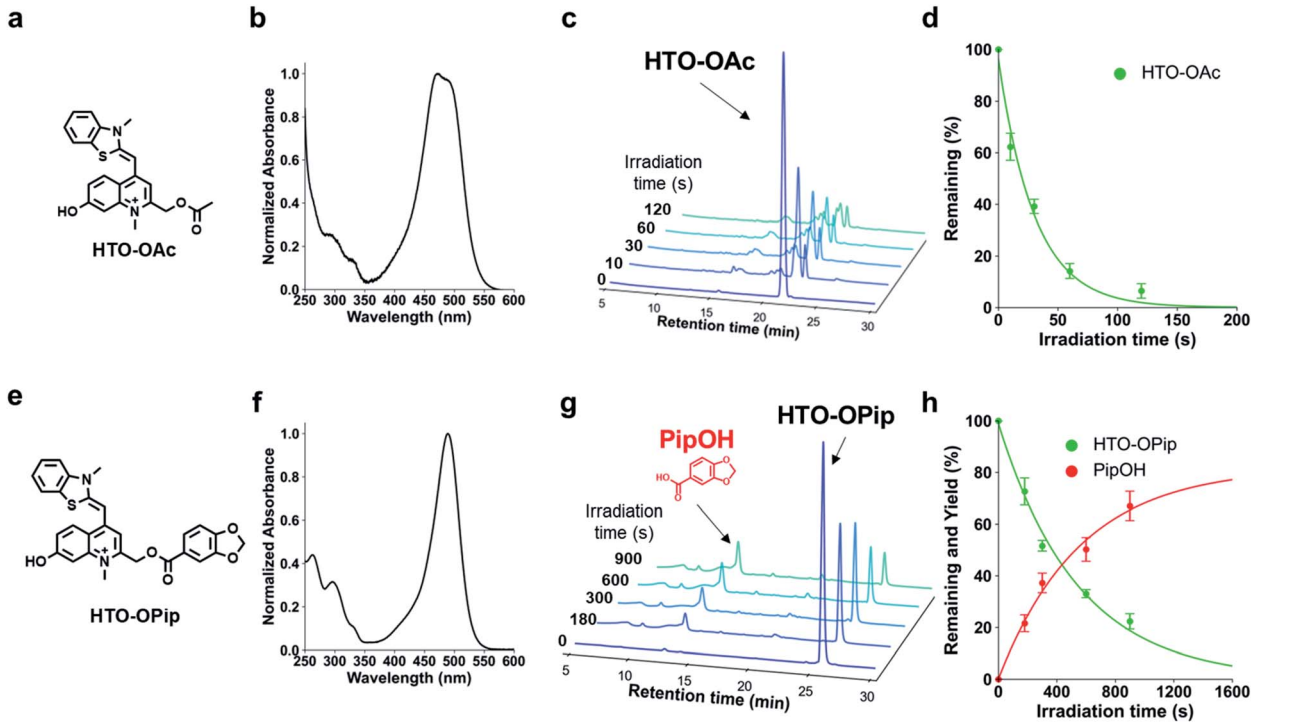

Fig. 2 The photochemical reaction of HTO-caged compounds. (a) Chemical structure of **HTO-OAc**. (b) Normalized absorption spectrum of 10 μM **HTO-OAc** at 25 °C in pH 7.4 PBS buffer (10% DMSO). (c) HPLC time courses of photolysis of **HTO-OAc** at 500 nm. Conditions: 100 μM **HTO-OAc** in PBS buffer (10% DMSO), light intensity: 10 mW cm^{-2}, $\lambda_{ex} = 490 \pm 5$ nm. (d) Quantitative monitoring of the photolysis reaction of **HTO-OAc**. Error bars represent the SD ($N = 3$). (e) Chemical structure of **HTO-OPip**. (f) Normalized absorption spectrum of 10 μM **HTO-OPip** at 25 °C in pH 7.4 PBS buffer/CH_3CN = 1/1 (3% DMSO). (g) HPLC time courses of photolysis of **HTO-OPip** at 254 nm. Conditions: 100 μM **HTO-OPip** in pH 7.4 PBS buffer/CH_3CN = 1/1 (3% DMSO), light intensity: 10 mW cm^{-2}, $\lambda_{ex} = 490 \pm 5$ nm. Error bars represent the SD ($N = 3$). (h) Quantitative monitoring of the photolysis reaction of **HTO-OPip**. Error bars represent the SD ($N = 3$).

Table 1 Spectroscopic and photochemical properties of HTO-caged compounds

Compound	λ_{max} (nm)	ε (M^{-1} cm^{-1})	t_{90} (s)	Φ	$\varepsilon\Phi$
HTO-OAc[a]	493	43 000	69	8.6×10^{-3}	370
HTO-OPip[b]	490	50 000	1239	3.8×10^{-4}	19
Sul-HTO-Glu[c]	488	49 000	231	2.3×10^{-3}	110

[a] PBS buffer (10% DMSO). [b] PBS buffer : CH_3CN = 1 : 1 (3% DMSO). [c] PBS buffer (3% DMSO).

Sul-HTO-Glu in aqueous solution with green light led to rapid degradation of **Sul-HTO-Glu** (Fig. 3c). Glutamate was released at a maximum yield of 40%, likely due to a photoinduced side reaction, although this has not been confirmed (Fig. 3d and S9†). The uncaging cross section of **Sul-HTO-Glu** in aqueous solution was 110, which was sufficiently high for spatiotemporal control of neurotransmitters (Table 1). Moreover, this value ($\varepsilon\Phi$ = 110) is much higher than those of other green-light sensitive caged bioactive compounds ($\varepsilon\Phi$ = <50).[6,14]

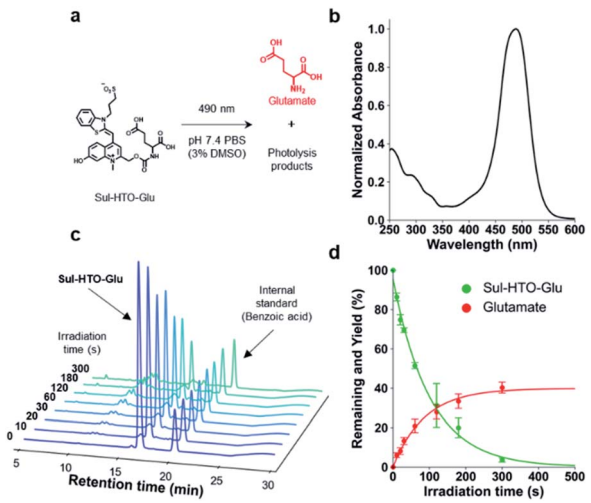

Fig. 3 Photolysis of **Sul-HTO-Glu** with 1PE. (a) Light-induced glutamate release from **Sul-HTO-Glu**. (b) Normalized absorption spectrum of 10 μM **Sul-HTO-Glu** at 25 °C in PBS buffer containing 0.1% DMSO (pH 7.4). (c) HPLC time courses of the photolysis of **Sul-HTO-Glu** at 254 nm. Conditions: 50 μM **Sul-HTO-Glu** and 300 μM benzoic acid as an internal standard in PBS buffer containing 3% DMSO (pH 7.4). Light intensity = 10 mW cm^{-2}, $\lambda = 490 \pm 5$ nm. (d) Quantitative monitoring of the reaction of **Sul-HTO-Glu**. Error bars represent the SD ($N = 3$).

2PE photolysis

1PE uncaging using visible/NIR light can be replaced by 2PE uncaging with NIR light. To investigate the 2PE uncaging cross

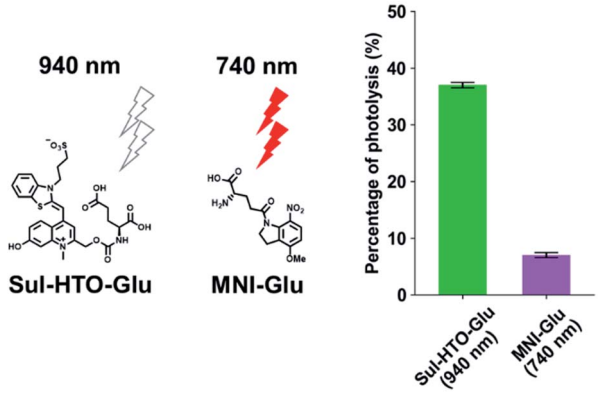

Fig. 4 Photolysis of **Sul-HTO-Glu** or **MNI-Glu** with 2PE. The percentages of **Sul-HTO-Glu** and **MNI-Glu** photolysis after 2PE for 1 h (**Sul-HTO-Glu**: 150 mW, λ_{ex} = 940 nm, **MNI-Glu**: 200 mW, λ_{ex} = 740 nm). Error bars represent the SD (N = 3).

sections of HTO-caged compounds, 2PE photolysis reactions with **Sul-HTO-Glu** were performed using a mode-locked Ti:sapphire laser and monitored by HPLC. Illumination of **Sul-HTO-Glu** at 940 nm for 1 h resulted in 37% of photolysis. The 2PE photolysis of **Sul-HTO-Glu** was evaluated by comparing 2PE photolysis with commercially available **MNI-Glu** at 740 nm. The percentage of **MNI-Glu** photolysis with 2PE was only 7% (Fig. 4). This result implies that **Sul-HTO-Glu** is more sensitive to 2PE than **MNI-Glu** despite using a longer wavelength for 2PE.

Activation of NMDA receptors by Sul-HTO-Glu with green light

To confirm the utility of these new green-light-sensitive HTOs in the biological setting, we attempted optical control of NMDARs in *Xenopus* oocytes and HEK293T cells using **Sul-HTO-Glu**. NMDARs are glutamate-gated ion channels that play important roles in learning and memory and may also be involved in various neurological and psychiatric disorders.[26] The binding of glutamate to the GluN2 subunits is required for full activation (Fig. S10†). We tested whether illumination of **Sul-HTO-Glu** could release glutamate under biological conditions and activate an ionic current by opening NMDAR channels (Fig. 5a). Ionic currents were recorded from *Xenopus* oocytes expressing NMDARs using a two-electrode voltage clamp. Following a 10 s waiting period after preapplication of **Sul-HTO-Glu**, 10 s illumination of the NMDAR-expressing oocytes using a 505 nm LED immediately evoked an inward current (Fig. 5b). As expected, illumination of NMDAR-expressing oocytes in the absence of **Sul-HTO-Glu** did not activate a current (Fig. S11†). Owing to its high water solubility and uncaging cross section, **Sul-HTO-Glu** achieved long-wavelength light activation with fast kinetics which is necessary for controlling neural activities. Ca^{2+} influx *via* NMDARs was also observed in HEK293T cells using a red fluorescent Ca^{2+} indicator, Calbryte 590. HEK293T cells

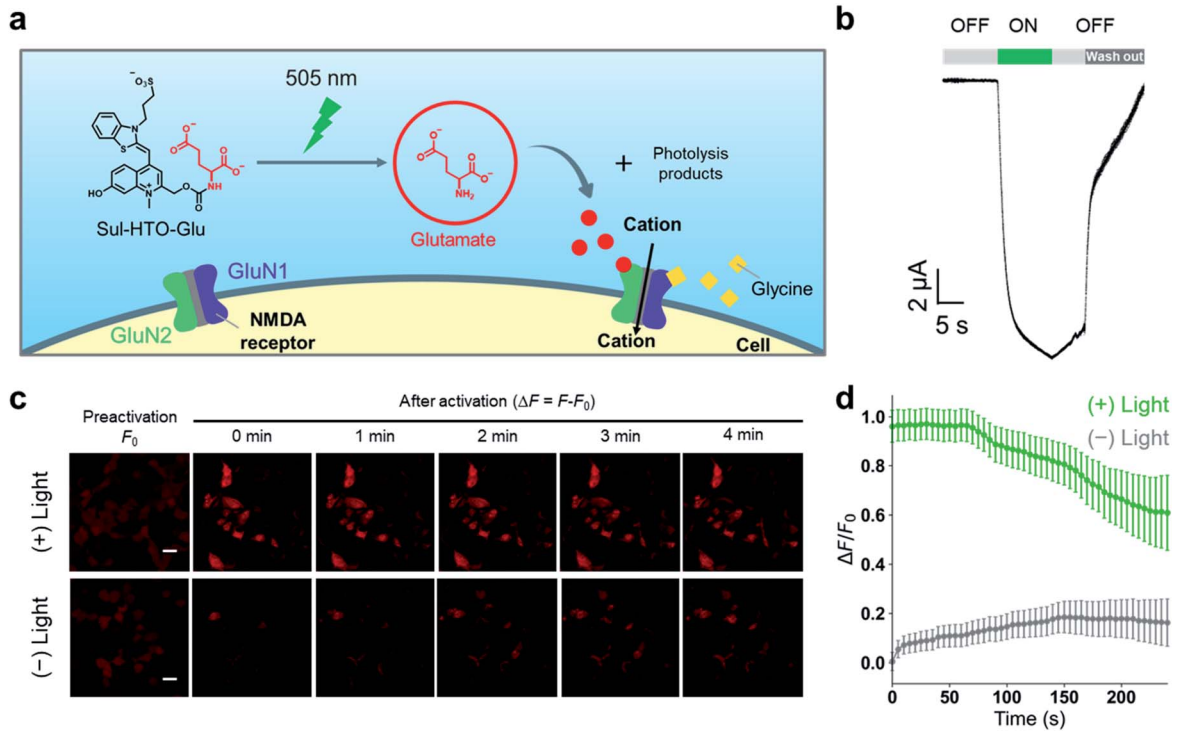

Fig. 5 Uncaging experiment of **Sul-HTO-Glu** in *Xenopus* oocytes and HEK293T cells. (a) The glutamate released from **Sul-HTO-Glu** by green light illumination binds to GluN2, which results in channel opening. (b) Release of glutamate to activate NMDARs in *Xenopus* oocytes upon green light photolysis with 100 μM **Sul-HTO-Glu** and 10 μM glycine in the pH 7.3 bath solution. Uncaging light was provided for 10 s (green bar). (c) Time lapse imaging of a red fluorescent Ca^{2+} indicator (Calbryte 590) with 559 nm excitation in HEK293T cells. Glutamate was uncaged upon green light photolysis with 25 μM **Sul-HTO-Glu** and 50 μM glycine (0.25% DMSO). Scale bar: 20 μm. (d) The fluorescence change after uncaging of glutamate. The fluorescence intensity was captured for every 5 s. Error bars represent SEM, n = 30 cells from two independent experiments.

expressing NMDARs were activated by applying glycine and glutamate (Fig. S12†). The calcium response was monitored on uncaging after HEK293T cells were loaded with **Sul-HTO-Glu** and glycine in the presence of Calbryte 590. A 10 s illumination using a 505 nm LED successfully evoked Ca^{2+} influx (Fig. 5c top row, Fig. 5d). On the other hand, the no-light condition did not evoke a Ca^{2+} response (Fig. 5c bottom row, Fig. 5d). Moreover, the fluorescence of **Sul-HTO-Glu** was not observed either inside or outside non-transfected HEK293T cells when excited at 473 nm (Fig. S13†). Importantly, **Sul-HTO-Glu** and the side products of illumination exhibited no cytotoxicity toward cultured HEK293T cells (Fig. S14 and S15†).

Conclusions

In conclusion, a new class of visible (one-photon) and near-infrared (two-photon) light-sensitive PPGs based on an HTO chromophore has been developed. The uncaging cross sections of HTO-caged compounds were superior to those of reported visible-light-responsive PPGs under aqueous conditions. Caged glutamate (**Sul-HTO-Glu**) was efficiently photolyzed by 2PE at 940 nm. These results demonstrate that HTO-caged compounds can immediately release biomolecules and activate target biological functions using visible/NIR-light illumination. Moreover, **Sul-HTO-Glu** was shown to activate NMDA receptors in *Xenopus* oocytes and mammalian HEK293T cells, which will enable its use in the optical control of neural circuits. We expect that the excellent optical properties of HTO will allow the control of biological functions in deeper tissues *in vivo*. The HTO light activation system can also be extended to a wide range of bioactive molecules such as drugs, peptides, and neurotransmitters. Furthermore, modification of HTO by replacing benzothiazole with other heterocyclic compounds enables the extension of the π-conjugate systems, which could provide long-wavelength visible/NIR-light-sensitive PPGs.[27]

Author contributions

R. Hashimoto, M. Minoshima, S. Sakata, H. Ishii, and Y. Watakabe performed the experiments. R. Hashimoto, M. Minoshima, S. Sakata, H. Ishii, and Y. Watakabe analysed the data. R. Hashimoto and M. Minoshima co-wrote the initial draft. R. Hashimoto, M. Minoshima, S. Sakata, F. Ono, H. Ishii, T. Nemoto, S. Yanaka, K. Kato, and K. Kikuchi revised the final manuscript.

Conflicts of interest

There are no conflicts to declare.

Acknowledgements

This research was supported by JSPS KAKENHI (grant numbers: JP17H06409 "Frontier Research on Chemical Communications" JP18H039351 and JP19K22255 to K. K.; 20K05747 and 21H00401 to M. M.; 20H05669 to T. N.; JP16H06280 "Advanced Bioimaging Support"), AMED (20ae0101041s0105 to K. K.; JP19dm0207078 to T. N.); the Platform Project for Supporting Drug Discovery and Life Science Research (Basis for Supporting Innovative Drug Discovery and Life Science Research (BINDS)) from AMED under grant number JP21am0101084; Joint Research of the Exploratory Research Center on Life and Living Systems (ExCELLS) (ExCELLS program no. 22EXC203); the Takeda Science Foundation (to K. K.); the Naito Foundation (to M. M.); the JSPS A3 Foresight Program; the JSPS CORE-to-CORE Program "Asian Chemical Biology Initiative"; the Japan (JSPS)-UK (RSC) Research Cooperative Program (JPJSBP120195705 to K. K.); and the JSPS-ISF Joint Research Program (JPJSBP120218404 to K. K.).

References

1 P. Klán, T. Šolomek, C. G. Bochet, A. Blanc, R. Givens, M. Rubina, V. Popik, A. Kostikov and J. Wirz, *Chem. Rev.*, 2013, **113**, 119–191.
2 P. Paoletti, G. C. R. Ellis-Davies and A. Mourot, *Nat. Rev. Neurosci.*, 2019, **20**, 514–532.
3 J. M. Silva, E. Silva and R. L. Reis, *J. Controlled Release*, 2019, **298**, 154–176.
4 E. Fino, R. Araya, D. S. Peterka, M. Salierno, R. Etchenique and R. Yuste, *Front. Neural Circuits*, 2009, **3**, 1–9.
5 N. G. Patil, N. B. Basutkar and A. V. Ambade, *Chem. Commun.*, 2015, **51**, 17708–17711.
6 N. Umeda, H. Takahashi, M. Kamiya, T. Ueno, T. Komatsu, T. Terai, K. Hanaoka, T. Nagano and Y. Urano, *ACS Chem. Biol.*, 2014, **9**, 2242–2246.
7 P. P. Goswami, A. Syed, C. L. Beck, T. R. Albright, K. M. Mahoney, R. Unash, E. A. Smith and A. H. Winter, *J. Am. Chem. Soc.*, 2015, **137**, 3783–3786.
8 J. A. Peterson, C. Wijesooriya, E. J. Gehrmann, K. M. Mahoney, P. P. Goswami, T. R. Albright, A. Syed, A. S. Dutton, E. A. Smith and A. H. Winter, *J. Am. Chem. Soc.*, 2018, **140**, 7343–7346.
9 A. P. Gorka, R. R. Nani, J. Zhu, S. Mackem and M. J. Schnermann, *J. Am. Chem. Soc.*, 2014, **136**, 14153–14159.
10 R. R. Nani, A. P. Gorka, T. Nagaya, H. Kobayashi and M. J. Schnermann, *Angew. Chem., Int. Ed.*, 2015, **54**, 13635–13638.
11 A. P. Gorka, T. Yamamoto, J. Zhu and M. J. Schnermann, *ChemBioChem*, 2018, **19**, 1239–1243.
12 R. R. Nani, A. P. Gorka, T. Nagaya, T. Yamamoto, J. Ivanic, H. Kobayashi and M. J. Schnermann, *ACS Cent. Sci.*, 2017, **3**, 329–337.
13 R. Weinstain, T. Slanina, D. Kand and P. Klán, *Chem. Rev.*, 2020, **120**, 13135–13272.
14 D. Kand, P. Liu, M. X. Navarro, L. J. Fischer, L. Rousso-Noori, D. Friedmann-Morvinski, A. H. Winter, E. W. Miller and R. Weinstain, *J. Am. Chem. Soc.*, 2020, **142**, 4970–4974.
15 M. Klausen and M. Blanchard-Desce, *J. Photochem. Photobiol., C*, 2021, **48**, 100423.
16 G. C. R. Ellis-Davies, *Front. Synaptic Neurosci.*, 2019, **10**, 1–13.

17 J. P. Olson, H. B. Kwon, K. T. Takasaki, C. Q. Chiu, M. J. Higley, B. L. Sabatini and G. C. R. Ellis-Davies, *J. Am. Chem. Soc.*, 2013, **135**, 5954–5957.
18 S. Ikeda, T. Kubota, M. Yuki and A. Okamoto, *Angew. Chem., Int. Ed.*, 2009, **48**, 6480–6484.
19 O. D. Fedoryak and T. M. Dore, *Org. Lett.*, 2002, **4**, 3419–3422.
20 M. Jarrett Davis, C. H. Kragor, K. G. Reddie, H. C. Wilson, Y. Zhu and T. M. Dore, *J. Org. Chem.*, 2009, **74**, 1721–1729.
21 T. Narumi, K. Miyata, A. Nii, K. Sato, N. Mase and T. Furuta, *Org. Lett.*, 2018, **20**, 4178–4182.
22 A. L. K. Hennig, D. Deodato, N. Asad, C. Herbivo and T. M. Dore, *J. Org. Chem.*, 2020, **85**, 726–744.
23 Y. Zhu, C. M. Pavlos, J. P. Toscano and T. M. Dore, *J. Am. Chem. Soc.*, 2006, **128**, 4267–4276.
24 J. Ma, A. C. Rea, H. An, C. Ma, X. Guan, M. De Li, T. Su, C. S. Yeung, K. T. Harris, Y. Zhu, J. L. Nganga, O. D. Fedoryak, T. M. Dore and D. L. Phillips, *Chem.–Eur. J.*, 2012, **18**, 6854–6865.
25 G. C. R. Ellis-Davies, *Acc. Chem. Res.*, 2020, **53**, 1593–1604.
26 S. F. Traynelis, L. P. Wollmuth, C. J. McBain, F. S. Menniti, K. M. Vance, K. K. Ogden, K. B. Hansen, H. Yuan, S. J. Myers and R. Dingledine, *Pharmacol. Rev.*, 2010, **62**, 405–496.
27 K. Ilina and M. Henary, *Chem.–Eur. J.*, 2020, 1–20.